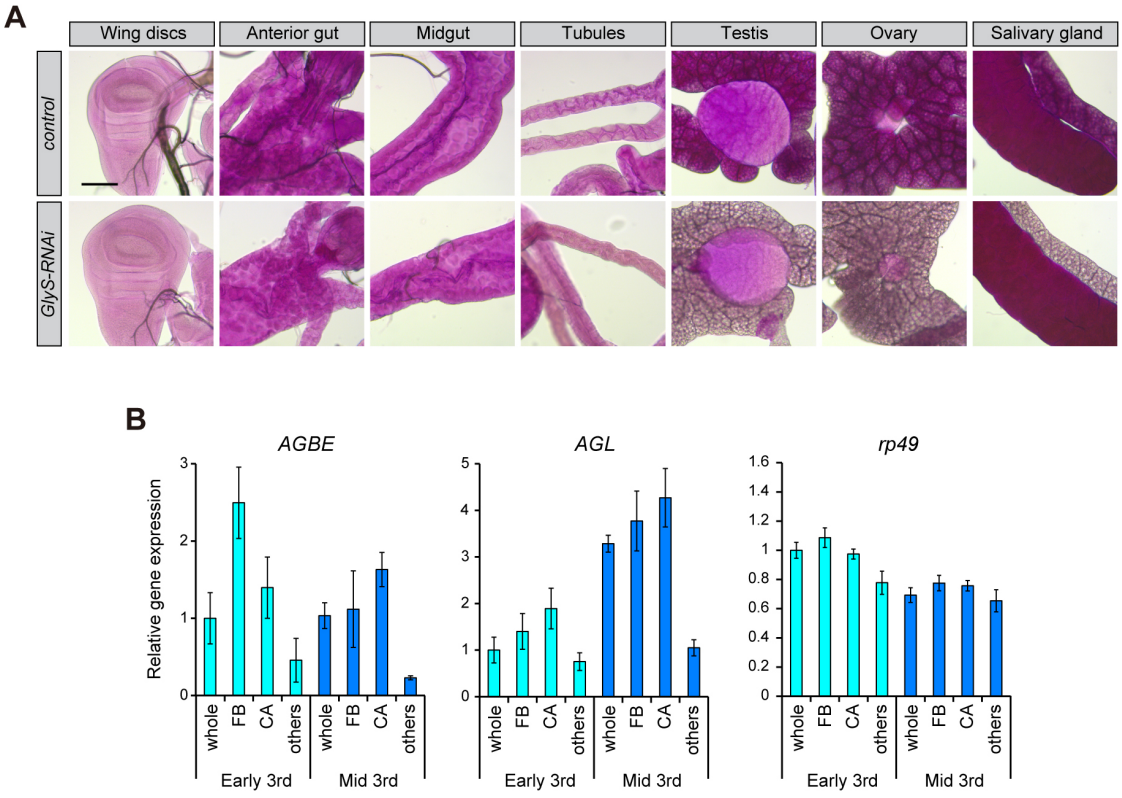

Figure S1. Tissue distribution and visualization of glycogen in larvae.

(A) PAS staining does not reliably detect stored glycogen in the imaginal discs, midgut, Malpighian tubules, testes, ovaries, or salivary glands under our experimental conditions. Stored glycogen was judged by the difference between control and *GlyS*-knockdown larvae. *Tub-Gal4* was used for ubiquitous knockdown. Of note, the results of PAS staining do not rule out the presence of glycogen in each tissue. Scale bars: 100 μm. (B) The tissue distributions of the gene transcripts related to glycogen metabolism were analyzed by qRT-PCR in early third-instar and mid third-instar larvae. whole, whole larva; FB, fat body; CA, carcass including body wall muscles; others, midgut and CNS. Relative changes in the *rp49* levels across tissues are also shown. The values shown are means and SD ($n = 4$).

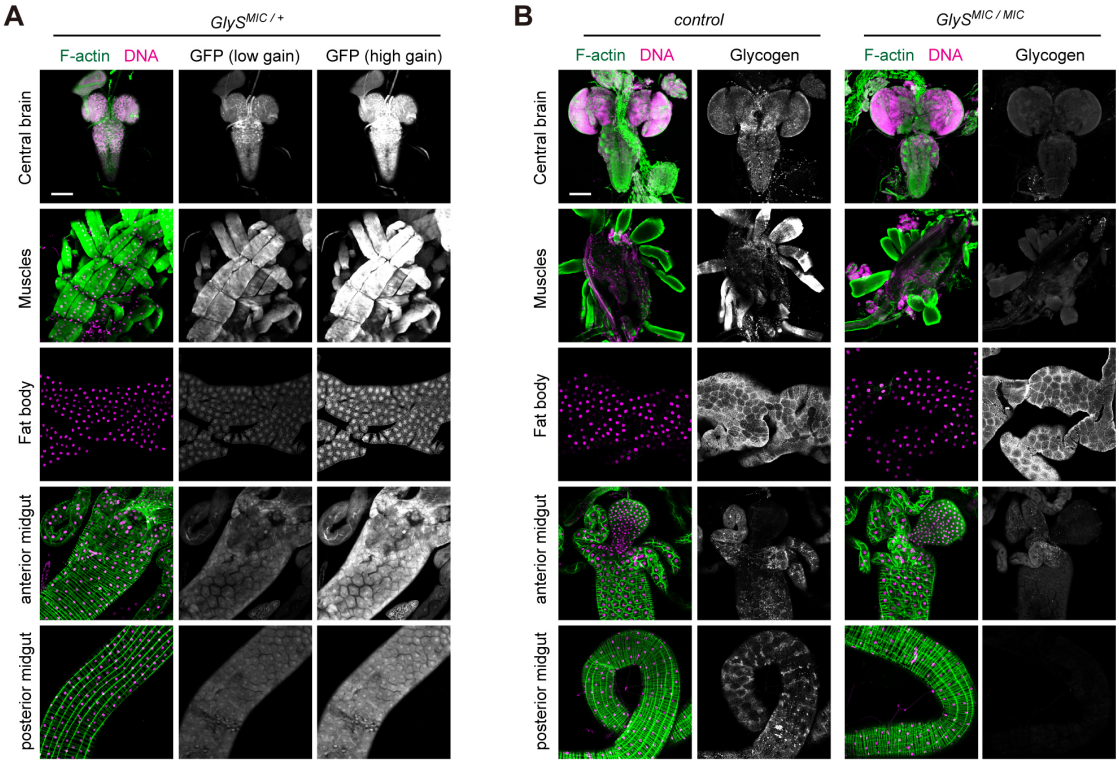

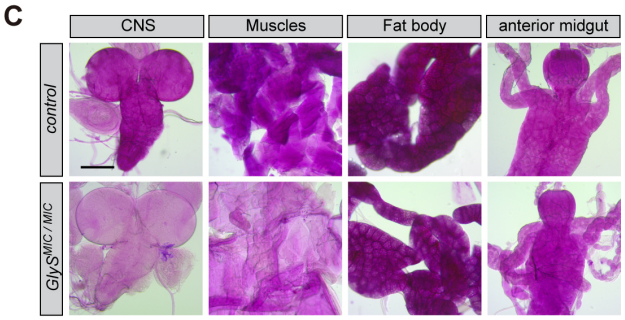

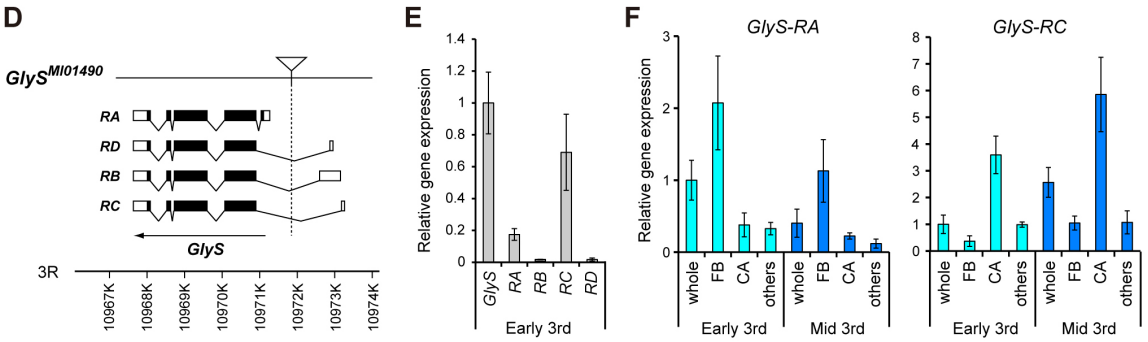

Figure S2. Characterization of a line with a *Minos* insertion in the *GlyS* gene locus. (A) GFP reporter expression of $GlyS^{MI01490}$ (named $GlyS^{MIC}$) was analyzed in each tissue. GFP expression is mainly detected in the muscles and CNS, and weak expression of GFP is detectable in the fat body and midgut. Two different imaging conditions are shown. (B) $GlyS^{MIC}$ homozygous mutants have significantly reduced amounts of glycogen in the brain, muscles, and midgut, but not in the fat body. Glycogen was visualized by immunostaining with anti-glycogen antibody. (C) Glycogen was visualized in each tissue by PAS staining. $GlyS^{MIC}$ homozygous mutants had significantly reduced brain glycogen and muscle glycogen, but the fat body glycogen was unaffected. Notably, glycogen stored in the midgut was accurately detected by immunostaining with anti-glycogen antibody, but not by PAS staining under these conditions. (D) Schematic representation of the *GlyS* locus. Protein-coding regions and untranslated regions are represented by black boxes and white boxes, respectively. The *Minos* insertion site, $GlyS^{MI01490}$, is marked with an inverted triangle. (E) Expression of *GlyS* transcripts in early third-instar larvae was analyzed by qRT-PCR. Serial dilutions of plasmids carrying cDNAs were used for standards. The relative expression levels are shown after the absolute quantification of mRNAs. (F) Tissue-dependent expression of *GlyS* transcripts was analyzed by qRT-PCR. The *GlyS-RA* transcript is mainly expressed in the fat body, whereas the *GlyS-RC* transcript is mainly expressed in the carcass, including the body wall muscles. whole, whole larva; FB, fat body; CA, carcass including body wall muscles; others, midgut and CNS. The values shown are means and SD. n = 4 [E, F]. Scale bars: 100 μm.

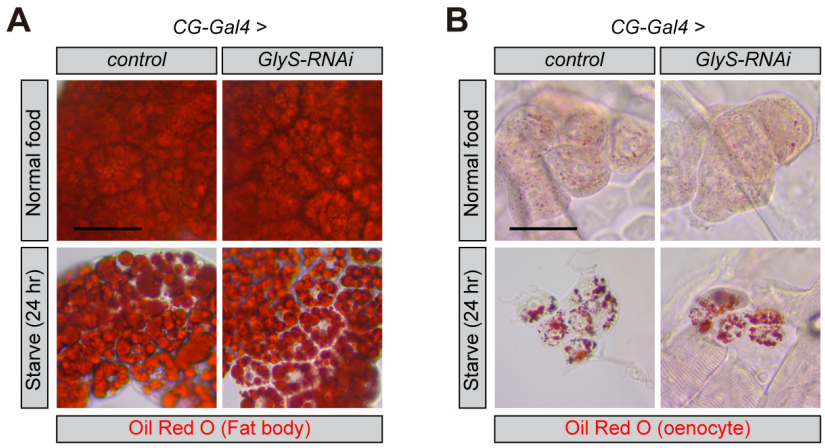

Figure S3. Loss of fat body glycogen does not significantly affect the mobilization of triglycerides.

(A) Knockdown of *GlyS* in the fat body does not affect the mobilization of lipid droplets in the fat body under starvation. (B) Knockdown of *GlyS* in the fat body does not affect the accumulation of lipid droplets in oenocytes upon starvation. Lipid droplets were visualized by Oil Red O staianing. Early third-instar larvae of the indicated genotypes were cultured on a normal food or agar-only diet for 24 hours. Scale bars: 50 μm.

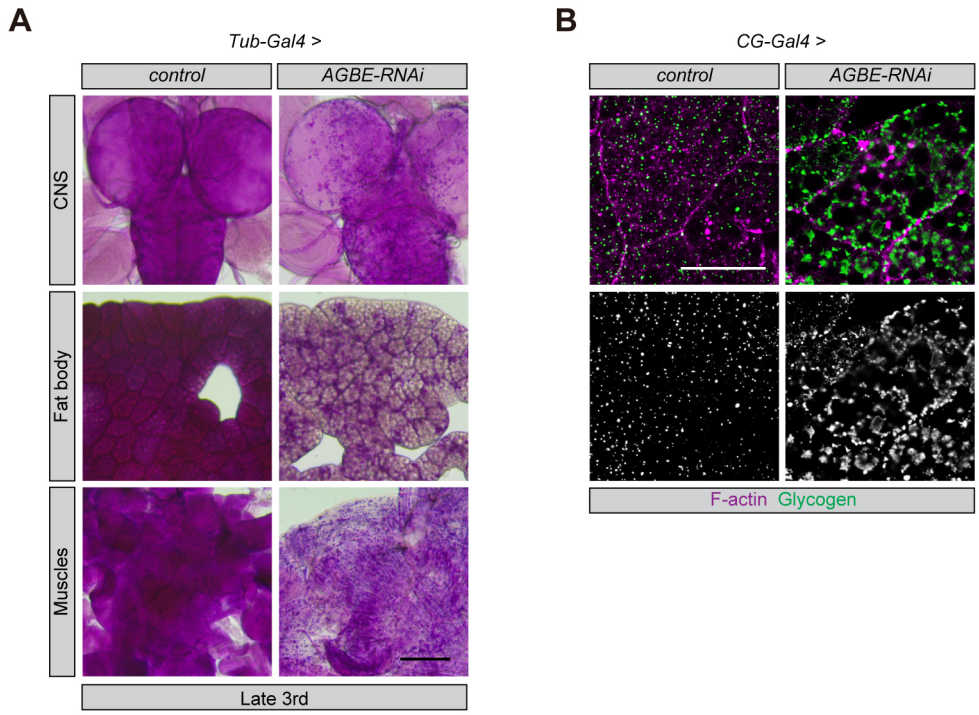

Figure S4. Knockdown of *AGBE* causes the aggregation of glycogen.

(A) Knockdown of *AGBE* causes the aggregation of glycogen. *Tub-Gal4* was used for ubiquitous knockdown. Glycogen in each tissue was visualized by PAS staining in late third-instar larvae. Scale bars: 100 μm. (B) Fat body glycogen was visualized by immunostaining with anti-glycogen antibody. Scale bars: 50 μm.

Figure S5. Sequence comparison of *Drosophila* GlyS and GlyP to mammalian GYS2 and PYGL.

(A) Amino acid sequence alignment of *Drosophila* GlyS and human liver glycogen synthase (GYS2). (B) Amino acid sequence alignment of *Drosophila* GlyP and human liver glycogen phosphorylase (PYGL). Identical and similar residues between the sequences are indicated by asterisks and colons, respectively. Blue colors indicate the amino acid sequence, which is unique in the *GlyS-RA* isoform. Red colors indicate the conserved phosphorylation sites, which regulate the enzyme activities. The amino acid sequence alignments were made using the ClustalW program. Human GYS2 RefSeq: NP_068776.2; Human PYGL RefSeq: NP_002854.3.

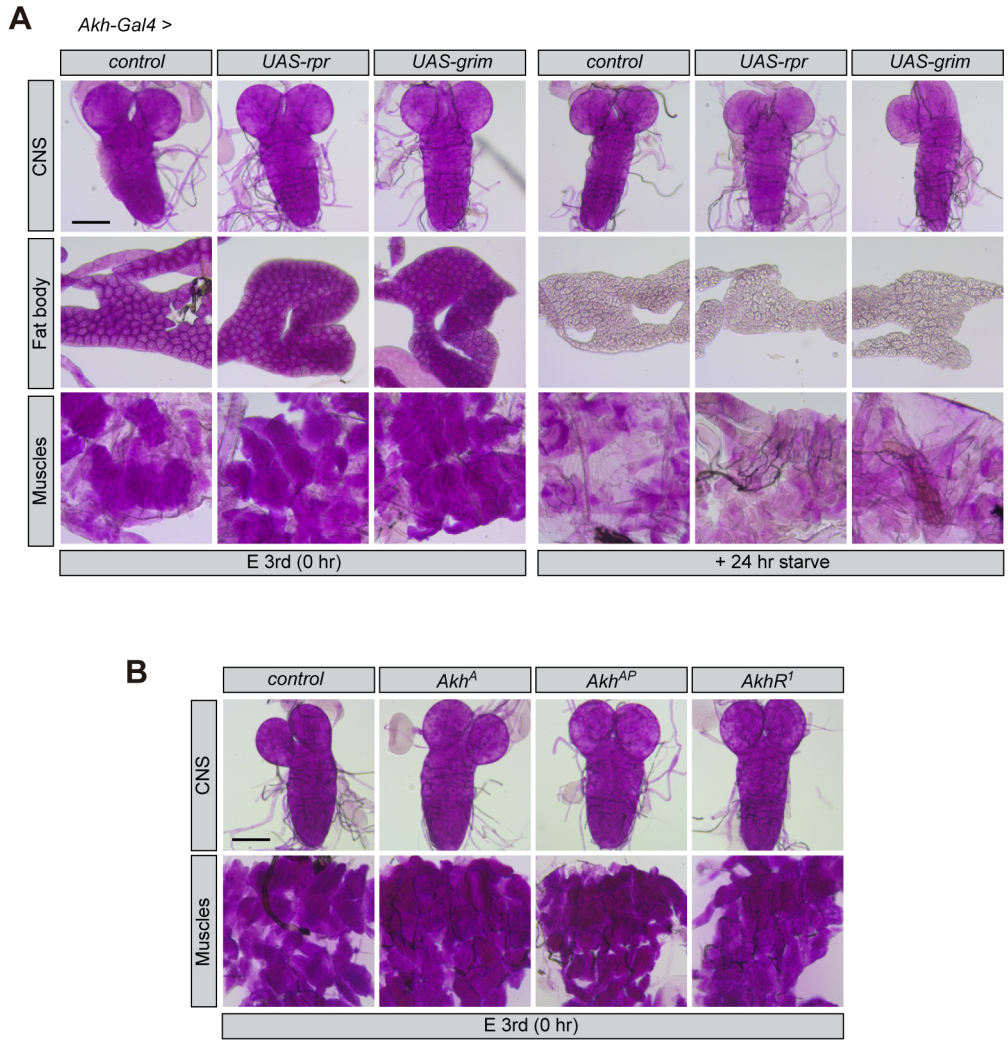

Figure S6. Akh signaling does not affect the steady-state levels or mobilization of muscle glycogen and brain glycogen in larvae.

(A) Loss of Akh-producing cells has no significant impact on the steady-state levels or mobilization of glycogen in muscles and the central nervous system (CNS). Glycogen was analyzed by PAS staining at the indicated time points. Early third-instar larvae (E 3rd) were used for the experiments. (B) The Akh^{A}, Akh^{AP}, and $AkhR^{1}$ mutants display no abnormalities at the steady-state levels of glycogen in muscles and the CNS. Scale bars: 100 μm.

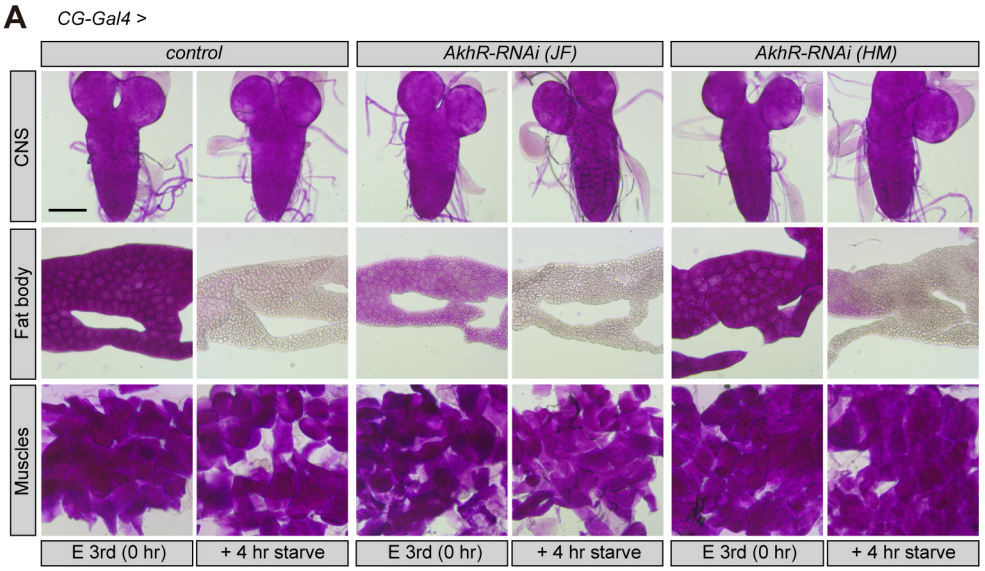

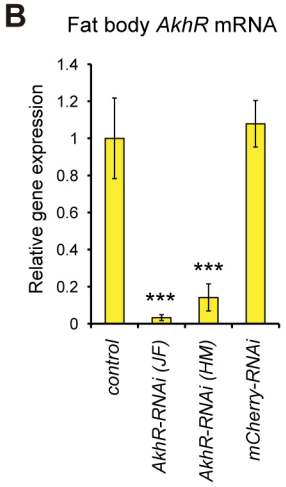

C

		Phenotype	Pupariation
CG-Gal4	*AkhR-RNAi (JF)*	viable	1 day delay
	AkhR-RNAi (HM)	viable	no delay
tub-Gal4	*AkhR-RNAi (JF)*	late pupal lethal	1∼2 days delay
	AkhR-RNAi (HM)	viable	no delay
Akh-Gal4	*UAS-rpr*	viable	no delay
	UAS-grim	viable	no delay

	Lethality	Pupariation
Akh^{A}	viable	no delay
Akh^{AP}	viable	no delay
$AkhR^{1}$	viable	no delay

Figure S7. Knockdown of *AkhR* in the fat body does not affect the mobilization of fat body glycogen.

(A) Steady-state levels and the mobilization of fat body glycogen were analyzed after knockdown of *AkhR* in the fat body. Although *AkhR-RNAi* (JF; BDSC#29577), but not *AkhR-RNAi* (HM; BDSC#51710), showed a decrease in the steady-state levels of fat body glycogen, mobilization after starvation occurred normally in both cases. Glycogen was analyzed by PAS staining at the indicated time points. Early third-instar larvae (E 3rd) were used for the experiments. Scale bars: 100 μm. (B) Knockdown of *AkhR* was confirmed by qRT-PCR in the dissected fat body from early third-instar larvae. The values shown are means and SD ($n = 4$). ***P<0.001; one-way ANOVA with Dunnett's post hoc test. (C) Summary of the *Akh* and *AkhR* mutants and *AkhR* knockdown

phenotype. Consistent with previous reports (Grönke et al., 2007; Gáliková et al., 2015), the Akh^{A}, Akh^{AP}, and $AkhR^{1}$ mutants display no lethality and no developmental delays under the standard diet conditions used in this study. Consistently, genetic ablation of the Akh-producing cells resulted in no lethality. It should be noted, however, that *AkhR-RNAi* (JF) displayed a growth defect and developmental delay when crossed with *CG-Gal4* and caused late pupal lethality (100% penetrance) when crossed with *tub-Gal4* under these conditions. *AkhR-RNAi* (HM) did not display such lethality upon ubiquitous expression. Therefore, *AkhR-RNAi* (JF) has off-target effect(s).

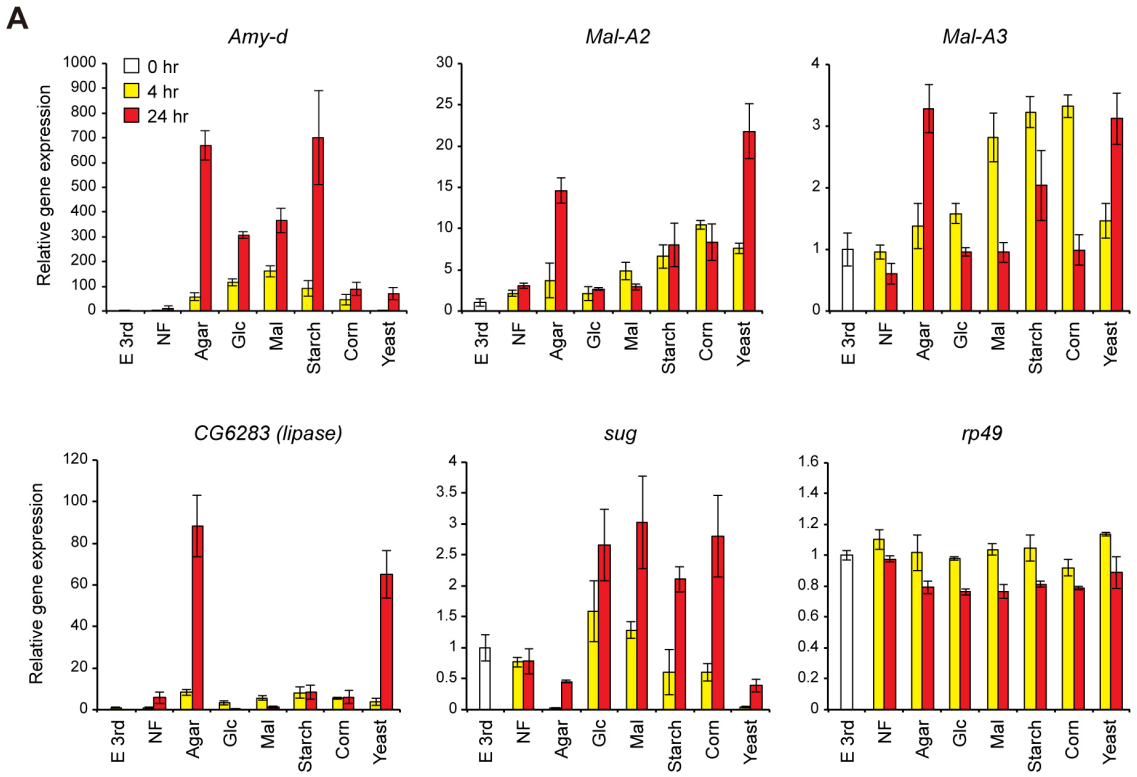

Figure S8. Changes in the expression level of digestive enzymes in larvae.

(A) The expression levels of digestive enzymes were analyzed by qRT-PCR under various dietary conditions. The feeding of a maltose-only (Mal), starch-only (Starch) or cornflour-only (Corn) diet induced the expression of maltase, namely, *Mal-A2* and *Mal-A3*, whereas the feeding of a glucose-only (Glc) did not. Continuous feeding of a maltose-only, starch-only or cornflour-only diet suppressed the further induction of *Mal-A2* and *Mal-A3*, whereas the continuous feeding of an agar-only (Agar) or a yeast-only (Yeast) diet up-regulated *Mal-A2* and *Mal-A3* in a time-dependent manner. The induction of an amylase, *Amy-d,* under starvation was in part suppressed by a glucose-only or maltose-only diet and strongly suppressed by a cornflour-only or yeast-only diet. Under these conditions, a sugar-responsive transcription factor, *sugerbabe* (*sug*), was up-regulated under carbohydrate-rich dietary conditions, while a digestive lipase, named *CG6283*, was induced under carbohydrate-poor dietary conditions. Of note, *Amy-d*, *Mal-A2*, *Mal-A3*, and *CG6283* are predominantly expressed in the midgut (Flybase). NF, normal food. The values shown are means and SD (n = 3). The relative changes in the *rp49* levels between conditions are also shown.

rp49 sense	CAGTCGGATCGATATGCTAAGCTG
rp49 antisense	TAACCGATGTTGGGCATCAGATAC
Tps1 sense	TCCGATGAGATCCTACAGGGTATG
Tps1 antisense	CGCCATGTTCCACCAGCAGATTG
Tret1-1 sense	ATGTCTCCGACATCGCCATGGTTC
Tret1-1 antisense	TCACCCATCATCAGCCAGGGAATG
GlyS sense	TTGCGCGATACGATCAACAACGTC
GlyS antisense	CGGATCATTCCAGTCATCAGCCAC
GlyP sense	CAACTGGTTGCTCTGAAGAAGTGG
GlyP antisense	CTGGCGCTTGTACTCGTGAATACG
AGBE sense	GCGAGGCGTACCTGAACTTTATGG
AGBE antisense	TCATTCATGGCTCGATCGAATTCG
CG9485/AGL sense	GCTTGACCATGCAGAGTGACAAGC
CG9485/AGL antisense	CGTAGATTGGCAAAGTTTAGCTCC
GlyS-RA sense	GATGCGCAGACAGCAGTCCTACCG
GlyS-RB sense	GTGAGATAGCACTTCATTTTCACC
GlyS-RC sense	TGTTTCGTGTGGCCAACAACAGCG
GlyS-RD sense	ACGGCAACAACAATTGATGAATCG
GlyS-RA/B/C/D common antisense	ACCGGATCACCGTGTAAATACCGC
Amy-d sense	TCAGAGTGAAATTTAGCTTCCACC
Amy-p sense	GAGTGAAACTGAACTTCCATCTGG
Amy-d/p common antisense	CCTTGACGGCGTTCTCGTTCACAG
Mal-A2 sense	TTCTAATTTCCACCACCCAGGAGG
Mal-A2 antisense	CATAAAAGTTAGAGATGTCGTAGC
Mal-A3 sense	TCAGTTCTACCAGATCTATCCCAG
Mal-A3 antisense	GGGCCTCGAAATCCTCCATTGTGC
Mal-A4 sense	ATGACCACTTGGACTAGCTTGTTC
Mal-A4 antisense	TGTCATAGCCAAAGTCTGCCATCG
CG6283 sense	TGCCGCCTTACTGGCAGCCGTGAG
CG6283 antisense	GAGCCGGACTTGGCCTTGATCTCC

Table S1.

Primers used for qRT-PCR analyses.